Biofabrication

International Society for Biofabrication

All-in-one biofabrication and loading of recombinant vaults in human cells

To cite this article: Fernando Martín *et al* 2022 *Biofabrication* **14** 025018

Biofabrication

PAPER

All-in-one biofabrication and loading of recombinant vaults in human cells

Fernando Martín[1,7], **Aida Carreño**[1,8], **Rosa Mendoza**[1,2], **Pablo Caruana**[3], **Francisco Rodriguez**[3], **Marlon Bravo**[4,5], **Antoni Benito**[4,5], **Neus Ferrer-Miralles**[1,2,6], **M Virtudes Céspedes**[3,*] and **José Luis Corchero**[1,2,6,*]

[1] Institut de Biotecnologia i de Biomedicina, Universitat Autònoma de Barcelona, Bellaterra, 08193 Barcelona, Spain
[2] CIBER de Bioingeniería, Biomateriales y Nanomedicina (CIBER-BBN), Bellaterra, 08193 Barcelona, Spain
[3] Grup d´Oncologia Ginecològica i Peritoneal. Institut d'Investigacions Biomédiques Sant Pau, Hospital de Santa Creu i Sant Pau, 08041 Barcelona, Spain
[4] Laboratori d'Enginyeria de Proteïnes, Departament de Biologia, Universitat de Girona, 17003 Girona, Spain
[5] Institut d'Investigació Biomèdica de Girona Josep Trueta, (IdIBGi), 17190 Salt, Spain
[6] Departament de Genètica i de Microbiologia, Universitat Autònoma de Barcelona, Bellaterra, 08193 Barcelona, Spain
[7] Present address: Nanobioengineering group, Institute for Bioengineering of Catalonia (IBEC), Helix building, C/ Baldiri Reixac 15-21, Barcelona 08028, Spain.
[8] Present address: Institut de Ciència de Materials de Barcelona, ICMAB-CSIC, Campus UAB, 08193 Bellaterra, Spain.
* Authors to whom any correspondence should be addressed.

E-mail: MCespedes@santpau.cat **and** jlcorchero@ciber-bbn.es

Keywords: vault particles, protein nanocages, drug delivery systems, self-assembling protein nanoparticles, eukaryotic cell factories

OPEN ACCESS

RECEIVED
9 February 2021

REVISED
15 February 2022

ACCEPTED FOR PUBLICATION
24 February 2022

PUBLISHED
9 March 2022

Abstract

One of the most promising approaches in the drug delivery field is the use of naturally occurring self-assembling protein nanoparticles, such as virus-like particles, bacterial microcompartments or vault ribonucleoprotein particles as drug delivery systems (DDSs). Among them, eukaryotic vaults show a promising future due to their structural features, *in vitro* stability and non-immunogenicity. Recombinant vaults are routinely produced in insect cells and purified through several ultracentrifugations, both tedious and time-consuming processes. As an alternative, this work proposes a new approach and protocols for the production of recombinant vaults in human cells by transient gene expression of a His-tagged version of the major vault protein (MVP-H6), the development of new affinity-based purification processes for such recombinant vaults, and the all-in-one biofabrication and encapsulation of a cargo recombinant protein within such vaults by their co-expression in human cells. Protocols proposed here allow the easy and straightforward biofabrication and purification of engineered vaults loaded with virtually any INT-tagged cargo protein, in very short times, paving the way to faster and easier engineering and production of better and more efficient DDS.

1. Introduction

Current therapies based on the administration of recombinant proteins in their native form usually face several drawbacks, such as short *in vivo* half-life, low membrane permeability, rapid elimination from blood stream, and undesired side effects caused by the multiple or high doses administered in order to reach the desirable concentration in the target cell or organ. As a result, these proteins need to be protected, typically by using nanocarriers that, at the same time, can be engineered to improve their targeted delivery to the desired biological site. In this line, a perfect nanocarrier should be able to deliver its cargo at the right moment, place and concentration. Thus, the use of smart drug delivery systems (DDSs), acting as a depot for high therapeutic concentrations and providing a solubilizing and protective environment is a promising strategy [1–3]. Nanoparticles (NPs) have been deeply explored as DDS, either for local release, where they are retained at the site of delivery, or for systemic delivery, increasing the circulation lifetime. NPs with self-assembly properties, good stability and specificity have already been used clinically

to provide targeted cellular/tissue delivery of chemotherapeutics, to improve drug bioavailability, to sustain drug effect in target tissue and for diagnostic purposes [4, 5].

Protein nano-DDSs are protein structures formed by the assembly of multiple copies of one or several different proteins. Nature already offers such functional macromolecular structures that can be easily manipulated for nanobiotechnology applications. Such naturally occurring structures, as virus capsids, bacterial microcompartments or ferritin cages, serve as excellent templates for functional biomaterials with precise architectures, unattainable by synthetic processes [3, 6, 7]. Advantages of protein NPs for drug delivery applications include their abundance in natural sources, biocompatibility, biodegradability, easy synthesis process, and cost-effectiveness. In contrast, other particulate systems like metallic NPs show several drawbacks like potential toxicity, large size, accumulation, or rapid clearance from the body. In addition, protein-based NPs offer the opportunity for surface modification by standard genetic engineering techniques, or by conjugation of other protein/s and carbohydrate ligands. The regular arrangement of protein subunits within protein cage structures allows for engineering of specific regions and surfaces (inner and/or outer) of the cage. Protein engineering has been extensively used to redesign structure and function, yielding particles with very narrow size distributions and multiple functionalities [8, 9]. In this context, eukaryotic vaults have emerged as an attractive nanocarrier for diverse types of biomolecules.

Vaults are ribonucleoprotein NPs large enough to encapsulate therapeutic molecules, and constitute a new and attractive approach for DDS as their use could reduce systemic side effects and immunogenicity. This feature, together with its homogeneity and versatility to be modified and specifically delivered to target cells, make vaults powerful nano-DDSs. These nanocapsules are the largest known ribonucleoprotein particles (∼40 × 70 nm, 13 MDa) found in eukaryotic cells. Vaults show a hollow, barrel-shaped structure with two protruding caps and an invaginated waist, based on a hierarchical protein self-assembly [10, 11]. Analysis of eukaryotic vaults revealed that each particle is composed by multiple copies of three proteins. Among them, the 'major vault protein' (MVP, 96 kDa) makes up 75% of the vault mass. Studies of recombinant vaults produced by MVP expression in insect cells confirmed that all the information needed to form the vault is encoded by this protein [12].

One interesting feature of vaults is their ability to encapsulate virtually any cargo protein, by two independent strategies: (a) fusing the cargo protein to the N-terminus of MVP protein or (b) fusing the cargo protein to the INT peptide (a vault targeting peptide from the C-terminus of the vault interacting protein VPARP) [13]. Moreover, it is possible to confer vaults specific targeting by adding a tag at the C-terminus of the MVP monomer. Such recombinant vaults expose these peptides on their exterior surface. This targeting strategy has been successfully applied to target cancerous cells [14]. Finally, vaults can be internalized *in vitro* via macropinocytosis or phagocytosis [15]. Taking into account all these properties, vaults have become one of the most promising nanovehicles as controlled DDS due to all their advantages (particle size, lumen large enough to encapsulate hundreds of protein molecules, protection of the cargo molecules from external proteases, biodegradability, biocompatibility, and non-immunogenicity). In this context, recombinant vaults have already been successfully explored for vaccination [16–18], proteins delivery [13, 19], targeting of cell surface receptors [14] and delivery of therapeutics for lung cancer [16] or glioblastoma [20].

Current production of recombinant vault NPs is mainly performed in *Spodoptera frugiperda* (*Sf*9) insect cells [12], where expression of only MVP protein is capable of directing the assembly of vault-like particles on polyribosomes [21]. However, this approach is complex and costly for industrial scale applications.

On the other hand, in order to develop an economically competitive platform based on recombinant vaults, efficient down-stream processes need also to be set-up and optimized, since vault size complicates its purification. Current vault purification protocol (based in several ultracentrifugation steps and additional gradient centrifugations) is complex, tedious and labor intensive [12]. Thus, much effort is being devoted to the development of faster and easier down-stream procedures for recombinant vaults, mainly focused in the substitution of centrifugation by special chromatographic columns.

In order to offer more efficient and fast up-stream and down-stream strategies for vaults production and purification, we describe in this work for the first time the production of recombinant vaults in human cells by means of transient expression of a His-tagged MVP protein (MVP-H6). This strategy also allows, by co-expressing MVP-H6 with INT-tagged cargo proteins, the spontaneous NPs biofabrication and their loading within the producing cell factory. Combined with the development of immobilized metal affinity chromatography (IMAC)-based purification methods, our approach renders a straightforward, 'all-in-one' procedure for easy and fast biofabrication of 'ready-to-use' loaded DDS.

2. Material and methods

2.1. Design, synthesis and cloning of recombinant genes

The sequence of the human major vault protein (MVP, UniProt Q14764, MVP_HUMAN) was used

to design the recombinant MVP-H6 gene. At the 3′ end of its native sequence, extra triplets encoding a six-histidine tag (6xHis) were added for further purification purposes. This sequence was cloned into the pTriEx1.1-Hygro vector (Novagen, cat. n° 70928-3, 6951 bp), between *Nco*I and *Eco*RI restriction sites. This expression vector enables optimal protein expression in bacterial, insect and mammalian cells from a single plasmid. The resulting plasmid pTriEx1.1-MVP-H6 encodes the protein MVP-H6, with 899 aminoacids in length and a molecular weight of 100.1 kDa.

With the aim of testing the putative encapsulation of a model protein within vault nanocapsules, an 'enhanced green fluorescence protein' (eGFP) was used. For that, the INT domain sequence was fused at the 3′ end of the eGFP gene. The INT domain is defined as the 163-aa region of the C-terminus (amino acids 1562-1724) of poly-(ADP-ribose) polymerase 4 (PARP4 protein, UniProt Q9UKK3, PARP4_HUMAN), which is the smallest region identified for PARP4 interaction with MVP protein in natural vaults. This GFP-INT sequence was also cloned into pTriEx1.1-Hygro vector between *Nco*I and *Eco*RI restriction sites. The resulting plasmid pTriEx1.1-GFP-INT encodes the protein GFP-INT, with 401 aminoacids in length and a molecular weight of 45.2 kDa.

All these genes were synthesized and cloned by GeneArt® (Life Technologies), and *Escherichia coli* DH5α strain was used for the maintenance and amplification of the expression plasmids.

2.2. Recombinant protein expression

Recombinant MVP-H6 and GFP-INT proteins were produced in a human cell line by transient gene expression (TGE). Briefly, the suspension-adapted human embryonic kidney (HEK) cell line FreeStyle 293F (Invitrogen, Life Technologies, ref R790-07) was used to produce the proteins by polyethylenimine (PEI)-mediated transfection and further TGE. Transfection conditions for this cell line had been previously set and optimized [22] at 1 μg DNA ml^{-1} of culture and a ratio DNA:PEI of 1:3 (w/w). Valproic acid (VPA) was added to cells (at 4 mM final concentration) 4 h post-transfection in order to improve recombinant protein expression. In co-expression experiments, both plasmids pTriEx1.1-MVP-H6 and pTriEx1.1-GFP-INT were mixed at different ratios (before their mixing with PEI), always maintaining the final amount of 1 μg plasmid DNA ml^{-1} and a ratio DNA:PEI of 1:3 (w/w).

To check protein expression, 1 ml samples from cultures were taken at different time-points after transfection, centrifuged (13 400 rpm, 10 min) and after that, supernatants were discarded. Cell pellets were resuspended in Laemmli buffer in order to analyze them by sodium dodecyl sulfate polyacrylamide gel electrophoresis (SDS-PAGE).

2.3. Cell fractionation

Cells were harvested, five days post-transfection (unless otherwise stated), by centrifugation (15 000 rpm, 10 min). Supernatants were discarded, and cell pellets were resuspended with phosphate buffered saline (PBS) supplemented with a protease inhibitor cocktail (cOmplete, EDTA-free, Roche Life Sciences, ref. 05056489001) and kept at −20 °C until cell lysis. To obtain soluble and insoluble fractions, samples were lysed by gentle sonication. Lysates were centrifuged (15 000 rpm, 15 min) and supernatants containing soluble proteins were separated from pellets (insoluble fraction), which were further resuspended in PBS.

2.4. SDS-PAGE and western blot analyses

To detect and quantify the recombinant proteins, SDS-PAGE was performed by using TGX Stain-Free™ FastCast™ acrylamide 12% (Bio-Rad, ref. 161-0185), and further visualization of proteins with a ChemiDoc™ Touch Imaging System (Bio-Rad). In some cases, further western-blot analyses were performed. To detect MVP-H6 protein, a rabbit polyclonal anti-MVP (Abcam, ref. Ab90009), or anti-His mouse monoclonal antibodies (from GenScript, ref. A00186-100, or from Clontech, ref. 631212), were used as primary antibodies. GFP-INT fusion protein was detected with an anti-GFP rabbit polyclonal (Santa Cruz Biotechnology, ref. sc-8334).

MVP-H6 protein amounts were densitometrically estimated by comparison, after SDS-PAGE and western-blot analyses, with known amounts of a control His-tagged protein produced and purified in-house, and quantified by the bicinchoninic acid (BCA) method. Samples and standards to be quantitatively compared were run in the same gel and processed as a set. Densitometric analyses of the immunoreactive bands were performed with the Image Lab™ software (version 5.2.1., Bio-Rad).

2.5. Protein purification

Purification of MVP-H6 protein was carried out from soluble fractions of transfected HEK 293F cells by commercial magnetic particles (MPs) ('Dynabeads His-tag isolation and Pull-down', Novex, Life Technologies, ref. 10103D), a platform based on IMAC chemistry. These MPs are superparamagnetic beads that use a cobalt-based IMAC chemistry to selectively capture His-tagged proteins. MPs were separated with a magnetic separator rack (New England Biolabs, ref. S1506S). Prior to purification, MPs were washed twice with PBS. Then, MPs were mixed with soluble fractions containing MVP-H6 and/or GFP-INT proteins, and incubated on a roller for 15 min at room temperature. After protein capture, MPs were magnetically immobilized and supernatant was collected (flow-through fraction, FT). Subsequently, MPs were washed with PBS, placed on the magnet and the supernatant collected as wash (W) fraction. Finally,

MVP-H6 protein was eluted from MPs with imidazole 500 mM in PBS and collected as eluted (EL) fraction. Eluted samples were dialyzed against PBS, used as storage buffer. Purified vaults were stored in PBS at 4 °C until use.

2.6. Physico-chemical characterization of recombinant vaults

Before transmission electronic microscopy (TEM), samples containing purified MVP-H6 were dialyzed in dialysis cassettes (Slide-A-Lyzer 3.5 K MWCO Dyalisis Cassettes, Thermo Scientific, ref. 66330) against buffer A (Tris-HCl 50 mM pH 8; NaCl 75 mM; $MgCl_2$ 0.75 mM). To visualize recombinant vaults through TEM, samples (5 μl) were prepared by absorption onto Cu-C grids for 2 min at room temperature. Following sample adsorption, grids were dried on filter paper, covered for 2 min with 5 μl of 2% uranyl acetate at room temperature and dried prior to viewing in a JEOL JEM 1400 microscope.

Size distribution of vault-based NPs was measured by dynamic light scattering (DLS) at 633 nm wavelength, combined with non-invasive backscatter technology in a DLS analyzer (Zetasizer Nano ZS, Malvern Instruments Ltd, Malvern, U.K.). Dispersions of purified NPs were filtered before DLS analysis to avoid putative interferences by remaining traces of MPs used for purification. Mean value of three measurements was taken as the hydrodynamic NP diameter.

2.7. GFP-INT protein expression and spontaneous encapsulation

Expression and spontaneous encapsulation of GFP-INT protein inside MVP-H6 based vaults was checked by co-transfecting HEK 293F cells with both pTriEx1.1-MVPH6 and pTriEx1.1-GFPINT expression vectors as described below. As controls, transfections with only one of the plasmids were performed. Five days post-transfection, recombinant proteins were purified following the magnetic procedure previously described. Finally, samples obtained during the process were submitted to SDS-PAGE and western blot analyses, developed with monoclonal Abs anti-His or a polyclonal Ab anti-GFP.

2.8. GFP-INT cell internalization mediated by recombinant vaults

Internalization of vaults loaded with GFP-INT in OVCAR-8 ovarian cancer cells was explored, by reproducing experiments described by Galbiati *et al* [23]. This cell line is representative of high-grade serous ovarian cancer, the most common and deadly form of ovarian cancer. OVCAR-8 cells (7.5×10^4) were seeded in a 24-well plate and incubated overnight with 0.5 ml Roswell Park Memorial Institute (RPMI) complete media. Then, they were treated with 12 nM GFPH6 or with recombinant vaults containing the same concentration of GFP-INT and incubated for 2 or 4 h at 37 °C in complete medium without phenol red. After incubation, cells were washed with cold PBS, trypsinized and centrifuged. Cells were resuspended in 0.5 ml of cold PBS and analyzed by flow cytometry. Ten thousand events were acquired in a Novocyte flow cytometer (Acea Biosciences, Inc.). Samples were analyzed using the NovoExpress software (Acea Biosciences, Inc.). Results are shown as mean and standard error of the mean (SEM) of two independent samples.

2.9. Cytotoxicity of recombinant vaults

Using the ovarian cancer model OVCAR-8 cell line, cytotoxicity of recombinant vaults was analyzed as follows. OVCAR8 cells were exposed for 48 h to different concentrations (up to 0.8 μM) of purified MVP-H6 vault-like structures. After that, cell viability was determined using the Cell Proliferation Kit II (XTT) (Roche, ref. 11465015001), following the manufacturer's specifications. Absorbance was measured at 450 nm on a spectrophotometer TECAM 2000. Data are expressed as cell viability relative (in percentages) to control cells (cells not exposed to recombinant protein). Results are shown as mean and SEM of two independent samples.

2.10. MVP-H6 protein stability in human serum

Stability of MVP-H6 NPs in human serum was also explored. For that, purified vaults were diluted in commercial human serum (Sigma, ref. S2257-5ML) and immediately incubated at 37 °C in a DLS analyzer. At different times (0, 5, 10, 15, 30 and 45 min) DLS measurements (by triplicate) were taken to follow NPs size. As controls, same experiment was performed but using phosphate buffer as vaults diluent or using vaults diluted in serum but kept at room temperature.

2.11. Statistical analysis

The normal distribution of the data was tested using the Kolmogorov-Smirnov test. Multiple comparisons with Kruskal–Wallis (SPSS software, version 19.0, IBM, New York, NY, USA) were used to compare cytotoxicity, and the pair-wise Student's *t*-test (Excel software, Microsoft Corporation), was used to compare NP internalization. The quantitative data of the experiments is reported as mean ± SEM. Differences among groups were considered significant at $p < 0.05$, and relevant divergences were labeled as $^{*}p < 0.05$, $^{**}p < 0.01$.

3. Results

3.1. MVP-H6 protein expression and solubility

Recombinant MVP-H6 protein was produced in HEK 293F cells by means of PEI-mediated transfection of plasmid pTriEx1.1-MVP-H6, and further TGE. Expression and accumulation of MVP-H6 into cells

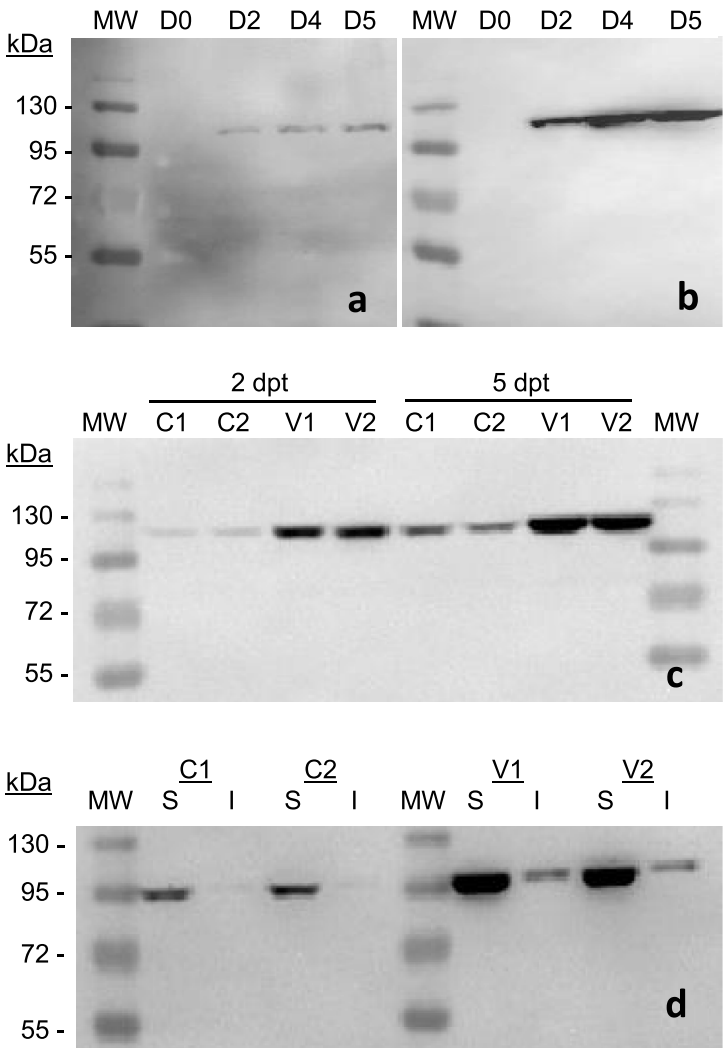

Figure 1. Expression levels and solubility of MVP-H6 protein expressed in HEK 293F cells. Expression of MVP-H6 protein in transfected HEK 293F cells (panels (a) and (b)) was monitored at days 0 (before transfection, D0) and two, four and five days post-transfection (D2, D4 and D5 lanes). Cells were analyzed by SDS-PAGE and further western blot detection with either a polyclonal antibody against MVP protein (panel (a)) or a monoclonal antibody anti-His tag (panel (b)). Effect of VPA on MVP-H6 expression was also checked (panel (c)). For that, duplicates of untreated (C1, C2) and VPA-treated (V1, V2) cultures taken two and five days post-transfection were analyzed by western blot developed with a monoclonal anti-His tag. Finally, effect of VPA on MVP-H6 solubility was explored (panel (d)) by comparing soluble (S) and insoluble (I) fractions of untreated (C1 and C2) of VPA-treated (V1 and V2) cultures taken 5 d post-transfection and analyzed by western blot developed with a monoclonal anti-His tag antibody.

were checked by SDS-PAGE and western-blot of total cell pellets taken at two, four and five days post-transfection, showing a progressive accumulation of the recombinant MVP-H6 protein within the cells (figures 1(a) and (b)). This protein, as expected, is recognized by antibodies directed to MVP protein (figure 1(a)) or to the His-tag (figure 1(b)), in a band corresponding to the expected MVP-H6 monomer of 100 kDa. In sample of day 0 (cells before transfection) no endogenous MVP protein is detected. This is indicative that, eventhough human cells contain endogenous MVP protein, they would only represent a small percentage (not detected by the anti-MVP protein antibody) compared to the amount of recombinant MVP-H6 protein.

In an attempt to improve protein yield, effect of VPA was checked. After analyzing total cell pellets of transfected cells taken at two and five days post-transfection, results showed that cultures treated with VPA produced 5.4- and 3.9-fold more protein than untreated cells, at two and five days post-transfection respectively (figure 1(c)). Solubility of any recombinant protein is of paramount importance regarding its putative application. For this reason, solubility of recombinant MVP-H6 protein was analyzed. HEK 293F cells were transfected and treated with VPA, or kept untreated as a control. Five days post-transfection, cell pellets were lysed and fractions analyzed by SDS-PAGE and further western blot. Results (figure 1(d)) showed that MVP-H6 protein is produced mainly in its soluble form. In untreated, control cells, 90.4 ± 0.9% of the protein remained within the soluble fraction, while in VPA-treated cells, the percentage of soluble MVP-H6 was of 86.2 ± 0.9%,

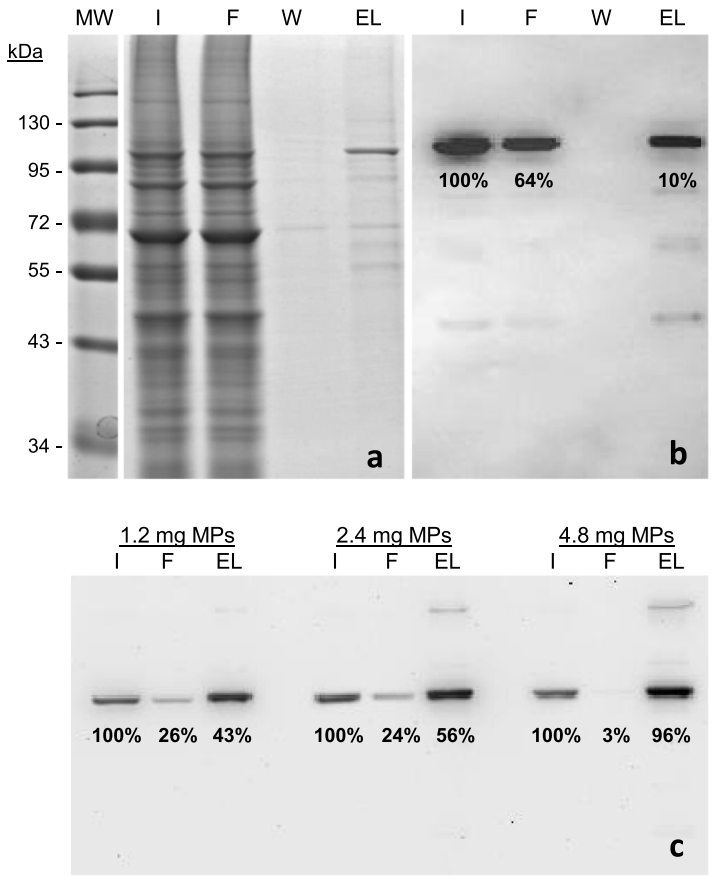

Figure 2. Magnetic purification of MVP-H6 protein. Initially, 1.2 mg of MPs and 40 μg of MVP-H6 (2 ml of initial sample, (I) were used. Flowthrough (F) and wash (W) fractions were also of 2 ml. Captured MVP-H6 was eluted (EL) in a final volume of 0.5 ml. Samples were analyzed by SDS-PAGE and TGX visualization (panel (a)) and western blot developed with a monoclonal antibody against His-tag (panel (b)). To optimize the efficiency of the process, a second experiment (panel (c)) was performed in which 30 μg of MVP-H6 protein were used as initial sample and mixed with 1.2, 2.4 or 4.8 mg of MPs. Samples were analyzed by western blot developed with a monoclonal antibody against His-tag. Numbers indicate the percentage of protein found in each sample according to densitometric analysis of the membranes.

indicating that increase in production due to VPA addition does not have a significant effect on protein solubility.

Finally, amounts of soluble MVP-H6 protein were estimated by western-blot. These amounts were of 20 ± 0.3 μg ml^{-1} or 86 ± 5 μg ml^{-1} in untreated or VPA-treated cells, respectively. VPA addition represents a 4.3-fold increase, in agreement with the previously detected increase. Taking all these results together, addition of VPA 4 h post-transfection was included in the production protocol for further experiments.

3.2. MVP-H6 protein purification

MVP-H6 protein was purified by means of MPs, using as starting material soluble fractions of transfected HEK 293F cells. In a preliminary experiment, soluble fraction containing 40 μg of MVP-H6 was mixed with 1.2 mg of MPs. Samples (initial, flow-through, wash and eluted) obtained during the process were analyzed by SDS-PAGE and western-blot (figure 2). TGX-based visualization (figure 2(a)) showed that MVP-H6 can be captured by MPs, and further eluted to a significant degree of purity. This indicates that His-tag is correctly expressed and exposed, and able to interact with metal ions on the MPs surface. In addition, no relevant proteins were detected in the 'wash' fraction, indicating that capture through the His-tag is highly specific. However, when analyzing the corresponding western blot (figure 2(b)), it was clear that a significant percentage of the initial MVP-H6 protein still remained in the 'flow-through' fraction, which indicates that the amount of MPs used was not enough to capture all the initial His-tagged protein. To address this issue and further improve the process efficiency, the experiment was repeated, mixing a constant initial amount of 30 μg of MVP-H6 protein with increasing amounts (1.2, 2.4 and 4.8 mg) of MPs. Under these conditions, 1.2 mg of MPs was again unable to capture the total amount of initial MVP-H6, rendering in the 'eluted' fraction only a 43% of the initial protein. However, when increasing the amount of MPs to 2.4 and 4.8 mg, percentages of MVP-H6 recovered increased to 56% and 96%, respectively (figure 2(c)). Taking all these results together, we could estimate that 5 mg of

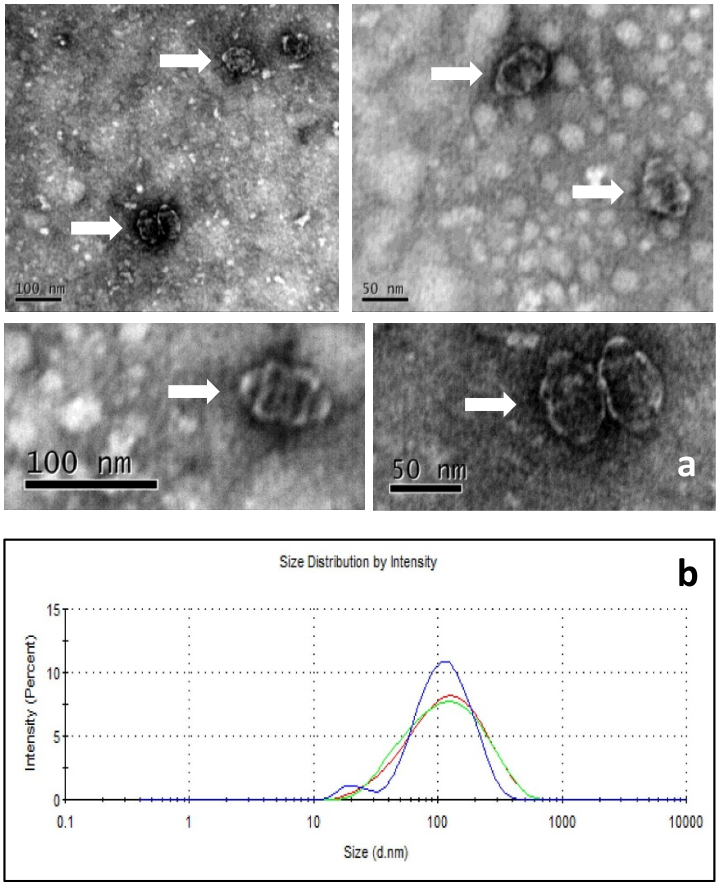

Figure 3. Nanoarchitecture of MVP-H6 based vaults. Transmission electron microscopy (TEM) micrographs (panel (a)) and DLS (panel (b)) of magnetically purified MVP-H6 protein. Both techniques show that MVP-H6 monomers self-assemble rendering nanocages with size (between 70 and 90 nm according to microscopy images) and shape (barrel) indistinguishable from that of native vaults or recombinant vaults expressed in other cell factories.

MPs should be able and enough to capture 30 μg of MVP-H6 protein, with a high degree (>85%) of purity.

3.3. Physico-chemical characterization of recombinant vaults

Purified MVP-H6 protein was visualized by TEM to check if this protein displays self-assembly properties and form vaults (or 'vault-like' structures). Results (figure 3(a)) confirmed the presence of NPs, almost identical in shape (a barrel-like nanocage formed by two symmetrical halves) and size (~70 × 40 nm) to the native or to recombinant vaults produced either in insect cells [12] or in *Pichia* cells [24]. This result confirms that MVP-H6 monomer produced in mammalian cells is correctly folded and maintains its self-assembling properties to form vault NPs. The size of these nanocages was estimated by DLS (figure 3(b)). When checking the size distribution of samples, results showed the presence of one main peak (corresponding to more than 95% of the sample intensity). Moreover, data showed a unique, single exponential decay in the auto-correlation functions. Taken together, these results are indicative of the presence of a single, main population. The samples were highly monodisperse as determined by the low polydispersity indexes obtained (0.28 ± 0.007), also indicative of their suitability for DLS analysis. The mean hydrodynamic diameters of our vaults, expressed as zeta-average mean size (as the primary parameter obtained by the technique) were of 92 ± 0.7 nm.

3.4. GFP-INT protein expression

To determine if these NPs were able to encapsulate a cargo protein, the fusion protein GFP-INT was used as a model. For that, co-transfections of HEK 293F cells with plasmids pTriEx1.1-MVP-H6 and/or pTriEx1.1-GFP-INT were performed. In a first experiment, both plasmids were mixed at a ratio 1:1 (0.5 μg of each plasmid ml^{-1}, keeping the final amount of 1 μg DNA ml^{-1}). With this strategy, we wanted to check (a) the possibility to express both proteins simultaneously, and (b) the effect of the amount of each plasmid in the protein yield obtained. Cell pellets were collected five days post-transfection and analyzed by western-blot either with antibodies against His-tag or GFP proteins. Results (figures 4(a) and (b)) showed that both proteins are simultaneously produced when co-transfecting cells with both plasmids. Decreasing in a 50% the amount of each plasmid does not result in a directly proportional

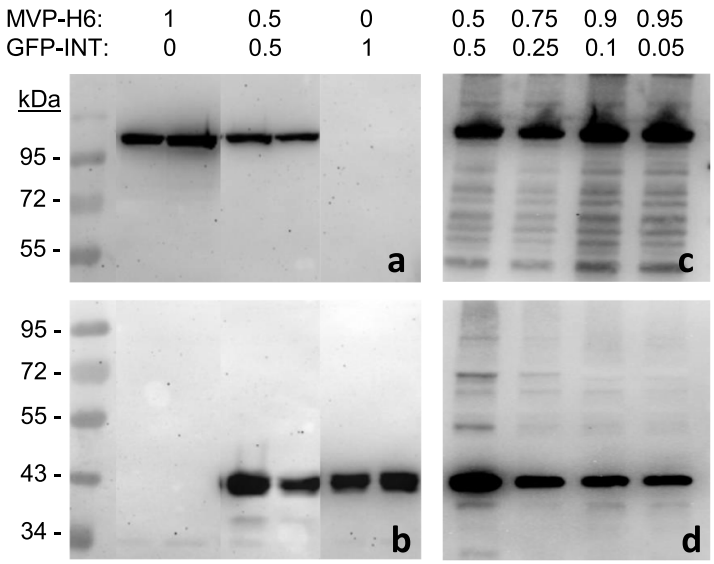

Figure 4. Co-expression MVP-H6 and GFP-INT proteins in HEK 293F cells. Co-expression of MVP-H6 and GFP-INT genes was driven by transfection of HEK 293F with the indicated concentrations of their respective plasmids (from 1 to 0.05 μg ml^{-1}). Five days post-transfection, cells were analyzed by SDS-PAGE and further western blot developed with either monoclonal antibodies anti-His tag (panels (a) and (c)) to detect MVP-H6 protein, or with a polyclonal antibody against GFP (panels (b) and (d)) to detect GFP-INT.

decrease in the yield of each protein: productions when co-expressing both proteins yielded >70% of each protein compared to controls (yields of protein expressed individually in single-plasmid transfections).

In a second experiment, we checked the possibility to further modulate the expression of each protein by varying plasmids ratio. For that, we increased amount of pTriEx1.1-MVP-H6 (from 0.5 to 0.95 μg ml^{-1}) and decreased amount of pTriEx1.1-GFP-INT (from 0.5 to 0.05 μg ml^{-1}). Results showed, again, that both proteins were correctly expressed simultaneously (figures 4(c) and (d)). Transfecting cells with only 0.05 μg ml^{-1} of plasmid pTriEx1.1-GFP-INT was enough to direct expression of GFP-INT protein at significant levels (31.6% compared to those obtained by transfecting cells with 0.5 μg ml^{-1}). Results of MVP-H6 protein (figure 4(c)) confirmed those of previous experiment: transfecting with only 0.5 μg of pTriEx1.1-MVP-H6 plasmid ml^{-1} still rendered >70% of protein compared to transfection using 0.95 μg of pTriEx1.1-MVP-H6 ml^{-1}.

3.5. Encapsulation and co-purification of GFP-INT protein

Soluble fractions from co-transfection experiments and controls (see above) were used to check the putative encapsulation of GFP-INT into vaults. For that, MVP-H6 protein was purified by using MPs, to check if GFP-INT protein was co-purified through its interaction (mediated by the INT peptide) with MVP-H6 protein. Samples of each fraction harvested during purification were analyzed by SDS-PAGE and western-blot (figure 5). Results from membranes developed with a monoclonal anti-His (figure 5(a)) showed that, as checked before, MPs used were enough to capture all the MVP-H6 protein present in the samples, that is further eluted by imidazol addition. Most important, the presence of GFP-INT did not interfere in the interaction of vaults with MPs, since vaults were correctly purified when GFP-INT was present in the initial sample.

On the other hand, results from membranes developed with a monoclonal anti-GFP (figure 5(b)) showed that when GFP-INT was expressed alone, it did not interact with MPs and was mainly found in the FT fraction. However, when both MVP-H6 and GFP-INT proteins were co-expressed and present in the initial sample, a significant percentage (54%) of GFP-INT was found in the eluted fraction. Since GFP-INT has no His-tag and therefore it cannot directly interact with MPs (as seen before), results indicate that GFP-INT protein was co-purified through its interaction with MVP-H6 protein.

However, almost 45% of GFP-INT protein still remained in the FT fraction, indicating that vaults present in the sample were not enough to encapsulate all the cargo protein. With the aim to improve the efficiency of the encapsulation process, purification protocol was repeated using a sample from a co-transfection in which plasmids pTriEx1.1-GFP-INT and pTriEx1.1-MVP-H6 had been used at 0.05 and 0.95 μg ml^{-1}, respectively. With this strategy, we expected to increase the ratio vault versus cargo protein, thus favoring the complete encapsulation of all the synthesized GFP-INT protein. Under these new conditions, cargo protein found in the FT fraction decreased to 14% (data not shown), corroborating

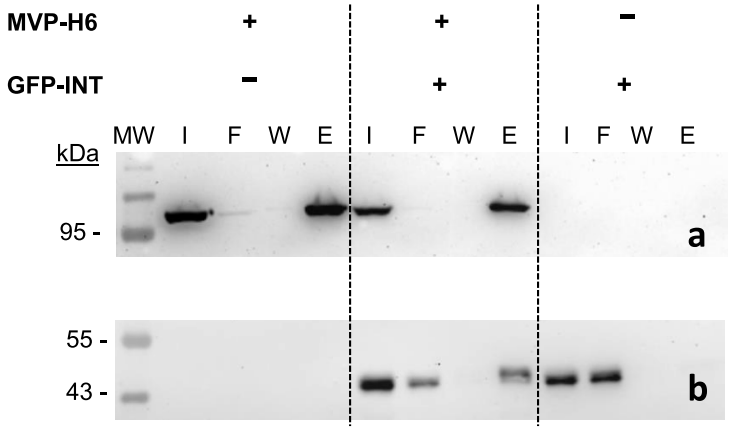

Figure 5. Co-purification of MVP-H6 and GFP-INT proteins in HEK 293F cells. Magnetic co-purification of MVP-H6 and GFP-INT proteins was performed as described in section 2. For each purification, initial (I), flowthrough (F), wash (W) and eluted (E) fractions were obtained and analyzed by western blot with a monoclonal antibody anti-His tag (panel (a)) or a polyclonal antibody against GFP (panel (b)). Symbols (+) and (−) indicate presence or absence of each protein in each sample.

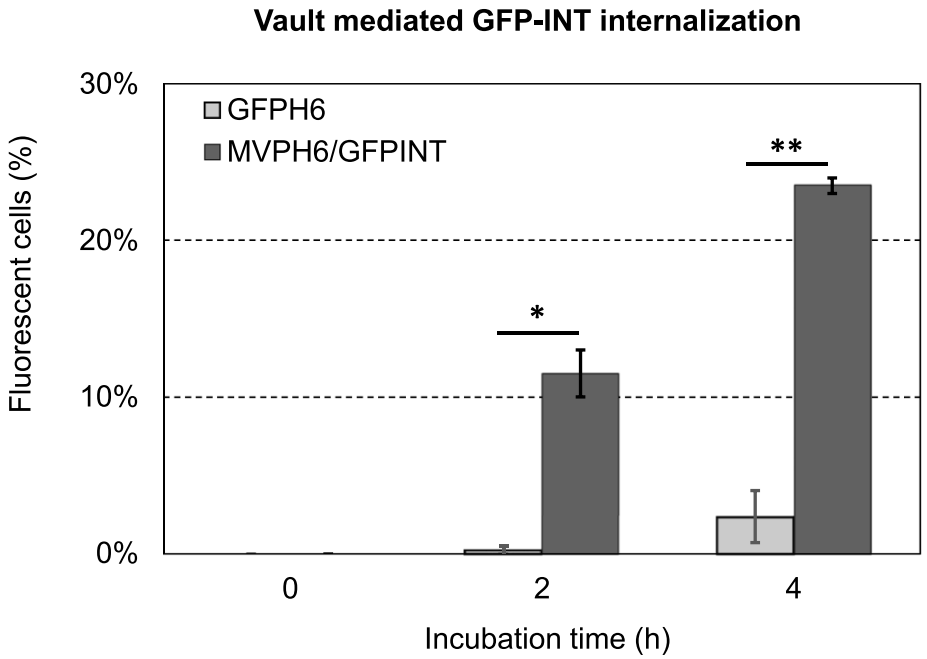

Figure 6. Cell internalization of GFP-INT mediated by vaults. The ability to internalize in OVCAR-8 cancer cells for a control protein GFPH6 (light grey bars) and for GFP-INT encapsulated within MVP-H6 based vaults (dark grey bars) was checked. Results showed here correspond to mean and SEM of two independent samples.

that after a careful adjustment and optimization of ratios vault/cargo protein, it should be possible to encapsulate within vaults all the cargo protein simultaneously produced within the cell factory.

Finally, we explored the amount of GFP-INT cargo protein entrapped by purified vaults. By means of SDS-PAGE and further western-blots (using as standards a commercial MVP protein and a recombinant GFP), we estimated that 1 mg of MVP-H6 protein self-assembled as vault could encapsulate approx. 15 μg of GFP-INT.

3.6. GFP-INT cell internalization mediated by recombinant vaults

The ability to internalize in cancer cells of a control protein GFPH6 and of GFP-INT encapsulated within MVP-H6 based vaults was checked by means of flow cytometry technique. Results (figure 6) showed that the control GFPH6 protein is hardly internalized into OVCAR-8 cells during the time of the assay. On the other hand, when the counterpart GFP-INT protein is encapsulated within vaults, it is able to internalize in a time-dependent fashion. According to this,

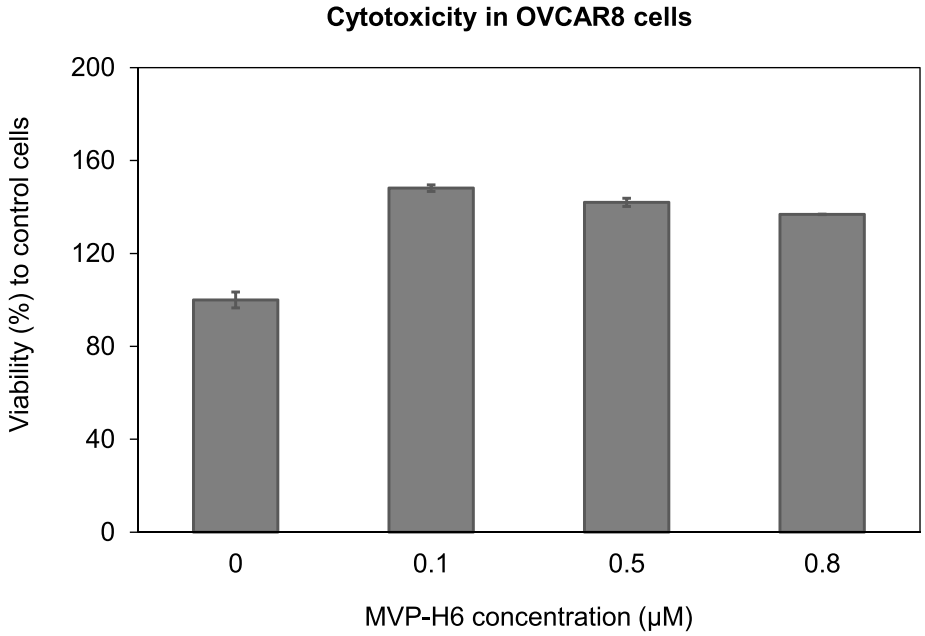

Figure 7. Vault cytotoxicity. Vaults cytotoxicity in OVCAR8 cancer cells was checked after 48 h of incubation with different MVP-H6 protein concentrations. Data are expressed as cell viability relative (in percentages) to control cells (cells not exposed to recombinant protein), and correspond to the mean and SEM of two independent samples.

the percentage of OVCAR-8 cells that become fluorescent due to GFP-INT internalization increases to approximately 12% and 24% after 2 and 4 h of incubation, respectively. This confirms the ability of vaults to enter cells (even without any specific cell targeting, as in our case) and thus, the well described functionality [16–20] of these nanocarriers as an efficient DDS.

3.7. Cytotoxicity of recombinant vaults

Cytotoxicity of MVP-H6 based vaults was checked by determining cell viability of OVCAR8 cells after their exposure for 48 h to different concentrations of recombinant MVP-H6 protein. Results (figure 7) showed no cytotoxic effect after 48 h of incubation, indicating that self-assembling process does not confer any toxicity to proteins that, like MVP-H6, are endogenous to human cells and, therefore, intrinsically innocuous.

3.8. Stability of recombinant vaults in human serum

Stability of MVP-H6 based vaults when incubated in human serum under physiological conditions was checked by following NPs size by DLS technique. Results (figure 8) showed that, when diluted in phosphate buffer, NPs basically remain unchanged and maintain their original hydrodynamic diameter. On the contrary, when incubated in human serum, two simultaneous phenomena seem to occur. In one hand, original structure (of about 195 nm, 'peak one') rapidly starts to dissociate, rendering a smaller particle of originally 42 nm of diameter ('peak 2'). On the other hand, and following incubation, both structures increase their hydrodynamic diameter up to 750 nm and 100 nm for peaks 'one' and 'two', respectively. Such sizes seem to stabilize and remain constant after 30–45 min of incubation at 37 °C. Interestingly, vaults diluted in human serum, but kept at room temperature, maintain their hydrodynamic diameter even after 45 min of incubation.

4. Discussion

Currently, many efforts are devoted to the development of new drug delivery strategies to overcome the shortcomings of ongoing drug-based therapies such as poor biocompatibility, lack of targeting specificity, inability to control release and low efficiency. In this context, eukaryotic vaults are a very promising DDS as they could overcome most, if not all, of these drawbacks.

Recombinant vaults are produced as empty protein nanocapsules and have been extensively explored in the last years as efficient DDS due to their biocompatibility, large inner lumen, simple composition (multiple copies of only one self-assembling protein), and the possibility (by means of easy, standard genetic engineering procedures) to tailor their sequence/structure. Recombinant vaults are currently produced in *Sf*9 insect cells [12], one of the few eukaryotic cells lacking endogenous vaults. This baculovirus-insect cell system is rather complex and costly for industrial scale applications. Obtention of a recombinant baculovirus requires tedious and time-consuming (3–6 months) processes, together with further growing, titration and maintenance of the baculovirus stocks. Moreover, continuous protein production is hampered by insect cell lysis during

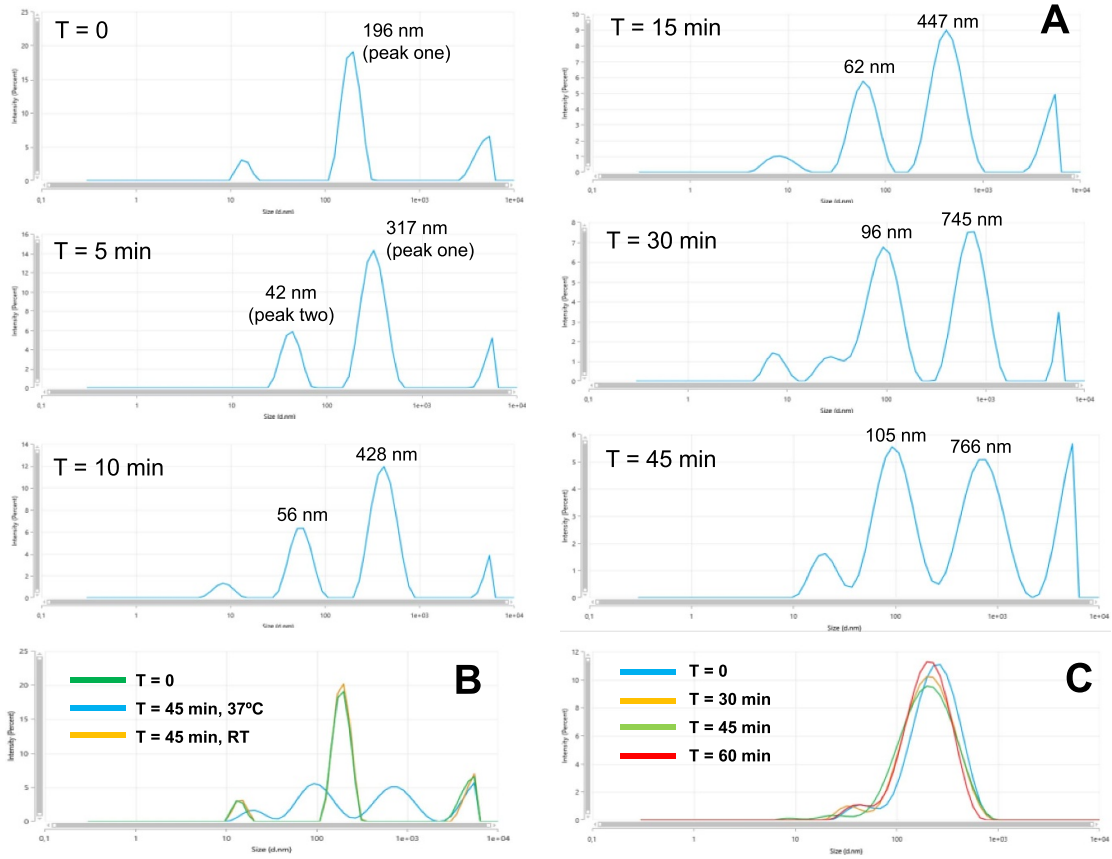

Figure 8. Stability of vault-based nanoparticles in human serum. Architectonic stability of vault-based nanoparticles in human serum at 37 °C was explored by DLS analysis. After dilution in human serum, DLS measurements were taken at different times (panel (A)). As controls, samples diluted in serum but kept at room temperature (panel (B)) and diluted in phosphate buffer at 37 °C (panel (C)) were also analyzed.

infection. Release of intracellular proteins from lysed cells, or removal or inactivation of progeny baculoviruses released by budding off from infected cells, may result in protein degradation by proteases and complicate the downstream process [25–27].

One significant change in the vault production process was the proposal of the replacement of the *Sf*9 insect cells for insect larvae, which allows higher productions [28], or the production of recombinant vaults in the yeast *Pichia pastoris* [24]. In these two alternative cell factories, expression of MVP alone also led to the formation of intact vaults, morphologically similar to endogenous vaults isolated from other eukaryotes. Nevertheless, due to a general unfamiliarity or restricted access to insect larvae culture, or putative immune response due to dissimilar post-translational modifications [29], these systems have not reached widespread popularity.

As a promising alternative, we propose the production of recombinant vaults in a human cell line (HEK 293F) by means of PEI-mediated transfection and further TGE. TGE is a well-suited strategy to fill this purpose, because of its ability to produce significant amounts of proteins within a short period of time [30, 31]. TGE involves short-term protein production (typically for up to ten days post-transfection) without further genetic selection of the encoding DNA [32]. Key TGE features are its simplicity and short time (normally, days) needed for the expression of the product, allowing the simultaneous study of many genes or their variants. This eukaryotic expression system provides fully homologous post-translational modifications to address biosafety concerns [33, 34].

In the present work, we have successfully produced a His-tagged MVP protein in HEK 293F cells by PEI-mediated transfection and further TGE. The protein was correctly produced and identified by antibodies against both MVP and His-tag domains. In our system, and after optimization of the protocol by VPA addition to transfected cells, MVP-H6 production reached (according to our preliminary studies) values of approx. 80 μg ml^{-1}, higher than those reported for *P. pastoris* (between 7 and 11 mg l^{-1}). No endogenous MVP protein was detected in non-transfected cells. This suggests that, even though human cells are known to contain endogenous MVP protein, this represents only a small percentage (not detected by the anti-MVP protein antibody) compared to the amount of recombinant MVP-H6 protein. In this line, a model has been described [21] for MVP synthesis and self-assembly

into vaults whereby the polyribosome acts like a 3D 'nanoprinter' to direct the ordered translation and assembly of the multi-subunit vault homopolymer, a process referred to as 'polyribosome templating'. According to this model, polyribosome would allow MVP monomers to self-assemble and form the vault structure within the crowded cytoplasm environment despite an extremely low overall monomer concentration. Taking all these results together, it is reasonable to predict that a single vault NP would be mainly composed by either endogenous MVP or by recombinant MVP-H6 protein, depending on the mRNA used as template in the polyribosomes. In this scenario, only vaults containing His-tagged MVP-H6 would be purified, since our down-stream process relies on platforms designed to capture His-tagged polypeptides, being endogenous, untagged vaults disregarded during this downstream process.

As described recently using the yeast *P. pastoris* as cell factory [24], expression of MVP-H6 in human cells also led to the formation of vault particles, with size (between 70 and 90 nm) and shape (barrel) indistinguishable from that of native vaults or recombinant vaults expressed in other cell factories. It is well known that NP size is a key parameter affecting applicability as DDS. Even within the nanoscale range, particle size strongly affects bioavailability and blood circulation time [35, 36]. Following systemic administration, particles with diameters below 10 nm are rapidly eliminated through extravasation and renal clearance [37], while particles with diameters greater than 200 nm are usually sequestered by the spleen and eventually removed by phagocytes [38]. Particles with diameters ranging from 10 to 70 nm can penetrate even very small capillaries [39], and particles with diameters ranging from 70 to 200 nm demonstrate the most prolonged circulation times [35]. Therefore, vaults produced in mammalian cells (as those expressed in other cell factories) would represent an excellent DDS candidate in terms of size parameter, since such NP dimensions (between 70 and 90 nm) fall within the optimal range described to interact with and internalize within target cells [40, 41]. Moreover, our TEM images showed the typical 'barrel' structure previously described for both natural and recombinant vaults. In this line, when cryoelectron microscopy and single-particle image reconstruction methods were used to determine the structure of nine recombinant vaults of various composition, all of them resulted in the typical vault 'barrel' structure, with a 48-fold rotational symmetry [42]. Also, cryo-tomography images of natural vaults in murine, simian and human cells were morphologically very similar, suggesting that vault structure is highly conserved among mammals [43]. Altogether, with such previous literature, our TEM and DLS results suggest that MVP-H6 proteins self-assemble spontaneously to form a recombinant vault very similar in architecture (if not exactly the same) and size than natural human vaults.

In the past, INT-tagged proteins have been successfully encapsulated within recombinant vaults by co-infection of *Sf*9 cells with recombinant baculovirus encoding MVP and the INT-tagged cargo protein [13]. Again, this approach needs the previous construction of the respective recombinant baculovirus. To overcome this drawback, we have co-expressed MVP-H6 protein with an INT-tagged GFP by co-transfection of HEK 293F cells with their respective encoding plasmids. As described previously [44], in TGE procedures a percentage of the encoding plasmid can be replaced with 'filler DNA' without a proportional reduction in the volumetric yield of the recombinant protein. In this line, our results indicate that the strategy presented here allows to co-express both MVP-H6 and INT-cargo proteins, and to modulate their yields by adjusting ratio of both encoding plasmids. Maintaining DNA total amount at 1 μg ml^{-1} during co-transfection, 0.05 μg ml^{-1} of GFP-INT encoding plasmid was still enough to produce significant amounts of this protein. By this 'all-in-one' approach, substitution of a small percentage of MVP-coding DNA by a plasmid encoding for INT-tagged cargo proteins renders an easy, fast and efficient way to encapsulate proteins with putative therapeutic or biotechnological applications.

Despite the increasing interest raised by vaults in the era of nanotechnology, current purification protocol is still rather complex and labor intensive [12], requiring three ultracentrifugation steps and two additional gradient centrifugations. Sucrose or cesium chloride gradient ultracentrifugation is generally considered appropriate for purification of different protein-based NPs, like virus-like particles (VLPs) [45, 46], but this approach is labor-intensive, time-consuming and scale-restricted [47], and can be associated with unexpected batch-to-batch variation. Although several reports have shown that gradient ultracentrifugation can be used for VLPs purification, it provided low yields and failed to remove impurities (including recombinant baculoviruses) from the final products [48]. Taking all these facts together, the need for the development of faster and easier down-stream procedures for recombinant vaults is clear, and much effort is being devoted to such purpose. A simpler procedure has been reported, which however requires baculovirus-infected insect larvae as starting material, not easily accessible to many research laboratories [28]. More recently, vault purification was proposed by means of a dialysis step and a subsequent size exclusion chromatography [23]. However, and despite all these efforts and advances, vault purification is still performed by the original protocol based on several ultracentrifugations.

In this line, another significant result of our study is the possibility to purify recombinant vaults by

means of magnetic procedures, in an attempt to substitute currently used vaults down-stream procedures. The application of magnetic separation techniques has received considerable attention in recent years. Magnetic separation is fast, gentle, scalable, easily automated, can achieve separations that would be impossible or impractical to achieve by other techniques, and have demonstrated credibility in a wide range of fields, including wastewater treatment, molecular biology, cell sorting or clinical diagnostics [49, 50]. The properties of MPs allow their selective manipulation and separation in the presence of other suspended solids, making possible to magnetically separate target proteins directly out from crude biological samples (e.g. fermentation broths, cell lysates, plasma, milk, whey or plant extracts). By this, the several stages of sample pretreatment (especially centrifugation, filtration and membrane separation) that are normally required to prepare samples before its loading onto packed bed chromatography columns, may be eliminated. It is also possible to integrate the disintegration and separation steps and thus shorten the total separation time [51]. Moreover, magnetic separation is usually very gentle to the target proteins or peptides. Even large protein complexes that tend to be broken up by traditional column chromatography techniques may remain intact when using more gentle magnetic separation procedures [52]. Finally, MPs can be used for protein concentration instead of ultrafiltration or precipitation techniques [53] in the cases where standard chromatography techniques render high volumes of diluted protein.

Following this rationale, we used commercial MPs to purify recombinant vaults from lysates of mammalian cells. This approach allowed us to obtain vaults with a high degree of purity (>85%) in a very short time by a fast, easy protocol. However, our results indicate that 5 mg of MPs would capture only 30 μg of MVP-H6 protein, a rather low capture efficiency compared to other purification systems like affinity chromatography. This issue need further study and optimization in the future if such magnetic strategy wants to substitute current downstream procedures for vault purification. Alternatively, innovative approaches based on affinity-based chromatography columns able to handle particles within the nanometric range could be explored in the future in order to substitute current vaults purification protocols. In this line, ion exchange columns Fractogel® EMD SO_3^- [54] or Fractogel® EMD TMAE followed by a polishing step by a gel filtration chromatography column (Superdex 200) [28] rendered final overall purities higher than 99%. Moreover, a two-steps protocol for vaults purification was recently described based on a dialysis step and further size exclusion chromatography [23].

By using magnetically purified vaults loaded with the cargo protein GFP-INT, we have demonstrated that recombinant vaults produced in human cells can deliver the cargo protein to cells, even in the absence of specific targeting peptides. These results confirm previous ones showing that non functionalized vaults are taken up unspecifically by HeLa [13, 14] and glioblastoma cell lines [23]. In the latter case, the process was demonstrated to be mediated by clathrin-mediated endocytosis. To improve cell internalization of recombinant vaults, their engineering by adding specific targeting peptides is one possibility that can be easily explored by the methods proposed here. Transfection of human cells and transient expression of engineered MVP proteins as proposed in this work is an easy and fast strategy to obtain recombinant vaults to be explored as new, improved DDS.

Finally, stability of vault-based NPs in human serum was addressed. Results show that vaults incubated at 37 °C in serum evolve from a monodisperse solution with one single NP population to the rapid appearance of some higher order structures, that stabilize after 30 min of incubation. Such higher ordered structures have already been observed and described in vaults resulting from the overexpression of MVP protein in insect cells [12]. Those ordered structures were referred to as 'vaultimers' and appeared to contain three to more than a dozen half-vaults. Moreover, these larger structures appeared to be enriched at higher sucrose concentrations in the gradient used for purification. In our case, when incubating purified vaults in a phosphate buffer also at 37 °C, formation of vaultimers was not detected. All these results could be indicative that complex matrixes or diluents might promote or facilitate vaultimers formation. However, diluent seems not to be the only factor affecting this phenomenon, since incubation in human serum but at room temperature does not result in vaultimers formation. The tendency of half-vaults to self-assemble into higher order structures is supported by the fact that the smaller structures (around 40 nm) initially appearing rapidly grow into bigger structures of up to 100 nm. Therefore, a combination of several factors (that should be further explored in detail in the future) seems to determine the final architecture of vault-based NPs.

5. Conclusions

In this work, we have produced for the first time in a human cell line recombinant NPs resulting from the self-assembly of a His-tagged MVP protein (main component of eukaryotic vaults), and a model protein (GFP-INT) could be encapsulated within such protein-based NPs. By using an approach combining MPs and western blot, we proved interaction of the INT-tagged GFP with vaults according to their co-purification profile. In addition, we have proved that GFP-INT cell internalization is clearly promoted when such protein is encapsulated within MVP-H6 based vaults, with no cytotoxicity detected for the nanovehicle. Altogether, these results prompt us to

propose human cells as cell factory, in combination with well-known TGE procedure, as a promising way to produce (in a very short period of time) significant amounts of recombinant vaults and variants of it. This all-in-one process in which nanovehicle and its therapeutic cargo are simultaneously produced provide a new promising approach to improve production processes. Such material can be an excellent tool for structural studies, or to develop improved DDS by addition of targeting peptides to the vault. Further work is still needed to optimize purification protocols of such new vehicles before they finally can be used as therapeutic DDS. In this context, large scale and reproducible particle purification methodologies need to be developed, together with the production of vaults under GMP, and the extensive toxicology, absorption, biodistribution, pharmacokinetics, and excretion studies required for all new drugs.

Data availability statement

All data that support the findings of this study are included within the article (and any supplementary files).

Acknowledgments

We acknowledge the financial support to our research in the field of vault nanoparticles as DDS received from Instituto de Salud Carlos III, through 'Acciones CIBER'. The Networking Research Center on Bioengineering, Biomaterials, and Nanomedicine (CIBER-BBN) is an initiative funded by the VI National R&D&I Plan 2008–2011, Iniciativa Ingenio 2010, Consolider Program, CIBER Actions and financed by the Instituto de Salud Carlos III with assistance from the European Regional Development Fund. The authors also appreciate the support of Spanish Ministerio de Ciencia, Innovación y Universidades and Instituto de Salud Carlos III through the Projects PI17/00553, PI17/00150, PI20/00770 and PI20/00623. Authors also acknowledge the financial support from Fundación Mutua Madrileña (FMMA) through project 'Targeted therapy for selective elimination of metastatic stem cells CXCR4+ in endometrial cancer' (AP1666942017), from Asociación Española Contra el Cancer (AECC) through project 'Development of an antitumor protein delivery system into ovarian cancer cells using the subcellular vault' (IDEAS18038BENI), and CIBER-BBN through the project 'Design of protein nanomedicines for targeted therapies in pancreatic cancer' (PANCREATOR). We also acknowledge the ICTS 'NANBIOSIS', more specifically the support from the Protein Production Platform of CIBER-BBN/IBB, at the UAB SepBioES scientific-technical service (www.nanbiosis.es/unit/u1-protein-production-platform-ppp/).

Conflict of interest

The authors declare no commercial or financial conflict of interest.

ORCID iDs

Fernando Martín https://orcid.org/0000-0002-3496-9093
Aida Carreño https://orcid.org/0000-0001-7725-7515
Rosa Mendoza https://orcid.org/0000-0002-0488-4814
Pablo Caruana https://orcid.org/0000-0002-0170-4355
Francisco Rodriguez https://orcid.org/0000-0001-7909-932X
Marlon Bravo https://orcid.org/0000-0002-0065-9812
Antoni Benito https://orcid.org/0000-0002-9776-1003
Neus Ferrer-Miralles https://orcid.org/0000-0003-2981-3913
M Virtudes Céspedes https://orcid.org/0000-0003-2956-5833
José Luis Corchero https://orcid.org/0000-0002-6109-144X

References

[1] Qi B, Wang C, Ding J and Tao W 2019 Editorial: Applications of nanobiotechnology in pharmacology *Front. Pharmacol.* **10** 1451
[2] McClements D J 2018 Encapsulation, protection, and delivery of bioactive proteins and peptides using nanoparticle and microparticle systems: a review *Adv. Colloid Interface Sci.* **253** 1–22
[3] Maham A, Tang Z, Wu H, Wang J and Lin Y 2009 Protein-based nanomedicine platforms for drug delivery *Small* **5** 1706–21
[4] Brigger I, Dubernet C and Couvreur P 2002 Nanoparticles in cancer therapy and diagnosis *Adv. Drug Deliv. Rev.* **54** 631–51
[5] Amreddy N, Babu A, Muralidharan R, Panneerselvam J, Srivastava A, Ahmed R, Mehta M, Munshi A and Ramesh R 2018 Recent advances in nanoparticle-based cancer drug and gene delivery *Adv. Cancer Res.* **137** 115–70
[6] Lee L A and Wang Q 2006 Adaptations of nanoscale viruses and other protein cages for medical applications *Nanomedicine* **2** 137–49
[7] Choi B, Kim H, Choi H and Kang S 2018 Protein cage nanoparticles as delivery nanoplatforms *Adv. Exp. Med. Biol.* **1064** 27–43
[8] Luo Q, Hou C, Bai Y, Wang R and Liu J 2016 Protein assembly: versatile approaches to construct highly ordered nanostructures *Chem. Rev.* **116** 13571–632
[9] Okesola B O and Mata A 2018 Multicomponent self-assembly as a tool to harness new properties from peptides and proteins in material design *Chem. Soc. Rev.* **47** 3721–36
[10] Tanaka H, Kato K, Yamashita E, Sumizawa T, Zhou Y, Yao M, Iwasaki K, Yoshimura M and Tsukihara T 2009 The structure of rat liver vault at 3.5 angstrom resolution *Science* **323** 384–8
[11] Tanaka H and Tsukihara T 2012 Structural studies of large nucleoprotein particles, vaults *Proc. Japan Acad.* B **88** 416–33
[12] Stephen A G, Raval-Fernandes S, Huynh T, Torres M, Kickhoefer V A and Rome L H 2001 Assembly of vault-like

particles in insect cells expressing only the major vault protein *J. Biol. Chem.* **276** 23217–20
[13] Kickhoefer V A *et al* 2005 Engineering of vault nanocapsules with enzymatic and fluorescent properties *Proc. Natl Acad. Sci. USA* **102** 4348–52
[14] Kickhoefer V A, Han M, Raval-Fernandes S, Poderycki M J, Moniz R J, Vaccari D, Silvestry M, Stewart P L, Kelly K A and Rome L H 2009 Targeting vault nanoparticles to specific cell surface receptors *ACS Nano* **3** 27–36
[15] Lai C-Y, Wiethoff C M, Kickhoefer V A, Rome L H and Nemerow G R 2009 Vault nanoparticles containing an adenovirus-derived membrane lytic protein facilitate toxin and gene transfer *ACS Nano* **3** 691–9
[16] Kar U K, Srivastava M K, Andersson A, Baratelli F, Huang M, Kickhoefer V A, Dubinett S M, Rome L H and Sharma S 2011 Novel CCL21-vault nanocapsule intratumoral delivery inhibits lung cancer growth *PLoS One* **6** e18758
[17] Kar U K *et al* 2012 Vault nanocapsules as adjuvants favor cell-mediated over antibody-mediated immune responses following immunization of mice *PLoS One* **7** e38553
[18] Champion C I *et al* 2009 A vault nanoparticle vaccine induces protective mucosal immunity *PLoS One* **4** e5409
[19] Wang M, Abad D, Kickhoefer V A, Rome L H and Mahendra S 2015 Vault nanoparticles packaged with enzymes as an efficient pollutant biodegradation technology *ACS Nano* **9** 10931–40
[20] Voth B L *et al* 2020 Intratumor injection of CCL21-coupled vault nanoparticles is associated with reduction in tumor volume in an *in vivo* model of glioma *J. Neurooncol.* **147** 599–605
[21] Mrazek J, Toso D, Ryazantsev S, Zhang X, Zhou Z H, Fernandez B C, Kickhoefer V A and Rome L H 2014 Polyribosomes are molecular 3D nanoprinters that orchestrate the assembly of vault particles *ACS Nano* **8** 11552–9
[22] Corchero J L, Mendoza R, Lorenzo J, Rodriguez-Sureda V, Dominguez C, Vazquez E, Ferrer-Miralles N and Villaverde A 2011 Integrated approach to produce a recombinant, His-tagged human alpha-galactosidase A in mammalian cells *Biotechnol. Prog.* **27** 1206–17
[23] Galbiati E, Avvakumova S, La Rocca A, Pozzi M, Messali S, Magnaghi P, Colombo M, Prosperi D and Tortora P 2018 A fast and straightforward procedure for vault nanoparticle purification and the characterization of its endocytic uptake *Biochim. Biophys. Acta* **1862** 2254–60
[24] Wang M, Kickhoefer V A, Rome L H, Foellmer O K and Mahendra S 2018 Synthesis and assembly of human vault particles in yeast *Biotechnol. Bioeng.* **115** 2941–50
[25] Fernandes F, Teixeira A P, Carinhas N, Carrondo M J T and Alves P M 2013 Insect cells as a production platform of complex virus-like particles *Expert Rev. Vaccines* **12** 225–36
[26] Kushnir N, Streatfield S J and Yusibov V 2012 Virus-like particles as a highly efficient vaccine platform: diversity of targets and production systems and advances in clinical development *Vaccine* **31** 58–83
[27] Vicente T, Roldão A, Peixoto C, Carrondo M J T and Alves P M 2011 Large-scale production and purification of VLP-based vaccines *J. Invertebr. Pathol.* **107** S42–S48
[28] Matsumoto N M, Buchman G W, Rome L H and Maynard H D 2015 Dual pH- and temperature-responsive protein nanoparticles *Eur. Polym. J.* **69** 532–9
[29] Walsh G and Jefferis R 2006 Post-translational modifications in the context of therapeutic proteins *Nat. Biotechnol.* **24** 1241–52
[30] Wurm F and Bernard A 1999 Large-scale transient expression in mammalian cells for recombinant protein production *Curr. Opin. Biotechnol.* **10** 156–9
[31] Pham P L, Kamen A and Durocher Y 2006 Large-scale transfection of mammalian cells for the fast production of recombinant protein *Mol. Biotechnol.* **34** 225–37
[32] Baldi L, Hacker D L, Adam M and Wurm F M 2007 Recombinant protein production by large-scale transient gene expression in mammalian cells: state of the art and future perspectives *Biotechnol. Lett.* **29** 677–84
[33] Hendriks I A, Lyon D, Young C, Jensen L J, Vertegaal A C O and Nielsen M L 2017 Site-specific mapping of the human SUMO proteome reveals co-modification with phosphorylation *Nat. Struct. Mol. Biol.* **24** 325–36
[34] Van Damme P *et al* 2012 N-terminal acetylome analyses and functional insights of the N-terminal acetyltransferase NatB *Proc. Natl Acad. Sci. USA* **109** 12449–54
[35] Ishida O, Maruyama K, Sasaki K and Iwatsuru M 1999 Size-dependent extravasation and interstitial localization of polyethyleneglycol liposomes in solid tumor-bearing mice *Int. J. Pharm.* **190** 49–56
[36] Kong G, Braun R D and Dewhirst M W 2000 Hyperthermia enables tumor-specific nanoparticle delivery: effect of particle size *Cancer Res.* **60** 4440–5
[37] Vinogradov S V, Bronich T K and Kabanov A V 2002 Nanosized cationic hydrogels for drug delivery: preparation, properties and interactions with cells *Adv. Drug Deliv. Rev.* **54** 135–47
[38] Stolnik S, Illum L and Davis S S 1995 Long circulating microparticulate drug carriers *Adv. Drug Deliv. Rev.* **16** 195–214
[39] Hawley A E, Illum L and Davis S S 1998 The effect of lymphatic oedema on the uptake of colloids to the lymph nodes *Biopharm. Drug Dispos.* **19** 193–7
[40] Shang L, Nienhaus K and Nienhaus G U 2014 Engineered nanoparticles interacting with cells: size matters *J. Nanobiotechnol.* **12** 5
[41] Jiang W, Kim B Y S, Rutka J T and Chan W C W 2008 Nanoparticle-mediated cellular response is size-dependent *Nat. Nanotechnol.* **3** 145–50
[42] Mikyas Y, Makabi M, Raval-Fernandes S, Harrington L, Kickhoefer V A, Rome L H and Stewart P L 2004 Cryoelectron microscopy imaging of recombinant and tissue derived vaults: localization of the MVP N termini and VPARP *J. Mol. Biol.* **344** 91–105
[43] Woodward C L, Mendonça L M and Jensen G J 2015 Direct visualization of vaults within intact cells by electron cryo-tomography *Cell. Mol. Life Sci.* **72** 3401–9
[44] Rajendra Y, Kiseljak D, Manoli S, Baldi L, Hacker D L and Wurm F M 2012 Role of non-specific DNA in reducing coding DNA requirement for transient gene expression with CHO and HEK-293E cells *Biotechnol. Bioeng.* **109** 2271–8
[45] Deo V K, Tsuji Y, Yasuda T, Kato T, Sakamoto N, Suzuki H and Park E Y 2011 Expression of an RSV-gag virus-like particle in insect cell lines and silkworm larvae *J. Virol. Methods* **177** 147–52
[46] Chung Y-C, Huang J-H, Lai C-W, Sheng H-C, Shih S-R, Ho M-S and Hu Y-C 2006 Expression, purification and characterization of enterovirus-71 virus-like particles *World J. Gastroenterol.* **12** 921–7
[47] Morenweiser R 2005 Downstream processing of viral vectors and vaccines *Gene Ther.* **12** S103–10
[48] Huhti L, Blazevic V, Nurminen K, Koho T, Hytönen V P and Vesikari T 2010 A comparison of methods for purification and concentration of norovirus GII-4 capsid virus-like particles *Arch. Virol.* **155** 1855–8
[49] Franzreb M, Siemann-Herzberg M, Hobley T J and Thomas O R T 2006 Protein purification using magnetic adsorbent particles *Appl. Microbiol. Biotechnol.* **70** 505–16
[50] Peter J F and Otto A M 2010 Magnetic particles as powerful purification tool for high sensitive mass spectrometric screening procedures *Proteomics* **10** 628–33
[51] Schuster M, Wasserbauer E, Ortner C, Graumann K, Jungbauer A, Hammerschmid F and Werner G 2000 Short cut of protein purification by integration of cell-disrupture and affinity extraction *Bioseparation* **9** 59–67

[52] Hofmann I, Schnölzer M, Kaufmann I and Franke W W 2002 Symplekin, a constitutive protein of karyo- and cytoplasmic particles involved in mRNA biogenesis in Xenopus laevis oocytes *Mol. Biol. Cell* **13** 1665–76
[53] de Dios Alché J and Dickinson H 1998 Affinity chromatographic purification of antibodies to a biotinylated fusion protein expressed in Escherichia coli *Protein Expr. Purif.* **12** 138–43
[54] Yang J, Srinivasan A, Sun Y, Mrazek J, Shu Z, Kickhoefer V A and Rome L H 2013 Vault nanoparticles engineered with the protein transduction domain, TAT48, enhances cellular uptake *Integr. Biol.* **5** 151–8